THE ASTROPHYSICAL JOURNAL, 207:1–15, 1976 July 1

THE SPECTRUM OF THE QSO PHL 957*

G. COLEMAN, R. F. CARSWELL, P. A. STRITTMATTER,† AND R. E. WILLIAMS
Steward Observatory, University of Arizona
AND
J. BALDWIN, L. B. ROBINSON, AND E. J. WAMPLER
Lick Observatory, Board of Studies in Astronomy and Astrophysics, University of California, Santa Cruz
Received 1975 October 23

ABSTRACT

Observations of PHL 957 have been made with the Steward Observatory echelette spectrograph and with the Lick Observatory image-tube scanner. The stronger emission lines are found to have markedly different profiles, making emission redshift determinations rather inaccurate. No He II λ1640 emission was detected. Wavelengths and approximate strengths of 203 absorption features are given, and two redshift systems ($z_A = 2.3088$, $z_K = 1.7969$) are shown to have a low probability of chance occurrence. Most of the lines observed shortward of emission Lα appear to be due to Lα in clouds of sufficiently low optical depth that Lβ is not detected. Systems *A* and *K* are similar in character to the absorption systems seen in 1331+170. The relative redshifts with respect to the emission systems are the same in the two QSOs and as such may provide evidence for Lyman line to Lyman continuum locking.

Subject headings: galaxies: redshifts — quasars

I. INTRODUCTION

PHL 957 ($m_v = 16.6$) is a radio-quiet quasar with an emission-line redshift $z_{em} \sim 2.69$ and with a rich absorption-line spectrum. An analysis of the absorption lines by Lowrance *et al.* (1972; hereinafter referred to as LMZOS) suggested 10 possible redshift systems, although a large number of lines still remained unidentified. The most striking feature of the spectrum of PHL 957 is an extremely strong absorption line at ~4020 Å identified as Lα in system *A* ($z_A = 2.309$). This feature was analyzed further by Beaver *et al.* (1972), who concluded that the line profile was consistent with that expected from a neutral-hydrogen column density $N_H \sim 10^{21}$ cm^{-2}. Further similarities between the system *A* absorption spectrum and that expected from a pure H I cloud were noted by Grewing and Strittmatter (1973), who suggested that this system may be the best presently known example of possible type II absorption, that is, of absorption arising in an intervening galaxy (Bahcall 1971). They also pointed out that, taken at face value, the LMZOS observations suggested a marked deficiency of metals relative to hydrogen in this system. Further observations of PHL 957 have been carried out by Wingert (1975) but with rather limited spectral coverage (3550–4500 Å) and signal-to-noise. High-quality spectra of this object have also been obtained by C. R. Lynds and provided the basis for a study of excited fine-structure level populations by Bahcall, Joss, and Lynds (1973).

Our own investigation of PHL 957 was undertaken in order (i) to check the high neutral-hydrogen column density in system *A* by observations of Lβ, (ii) to obtain high-resolution spectral data over a wider wavelength range to facilitate analysis of absorption line systems, and (iii) to study element abundances in both the emitting and absorbing regions of PHL 957.

II. THE OBSERVATIONS

Observations of PHL 957 were carried out both at Lick Observatory and at Steward Observatory at various times between 1972 and 1974. The Lick data were obtained with the image-tube scanner (ITS) system (Robinson and Wampler 1972), at the Cassegrain focus of the 3 m telescope. A summary of individual scan data is given in Table 1, and a sum of the 1972 and 1973 lower resolution scans covering the range 3100–9000 Å is shown in Figure 1. Emission-line strengths and widths for Lα, Si IV, C IV, and C III] are listed in Table 2 and will be discussed further in § III.

TABLE 1
LICK ITS OBSERVATIONS

Date	Scan Range (Å)	Resolution (Å)
1972 December 11.....	6408–8870	10
1972 December 13.....	4548–6848	10
1973 January 6.....	3360–5835	10
1973 January 31.....	3180–5542	10
1973 October 28.....	3068–5453	10
1973 October 29.....	6482–8942	10
1974 July 21.....	3150–4280	4
1974 July.....	3146–4271	4

* Lick Observatory Bulletin No. 711.
† Alfred P. Sloan Foundation Research Fellow.

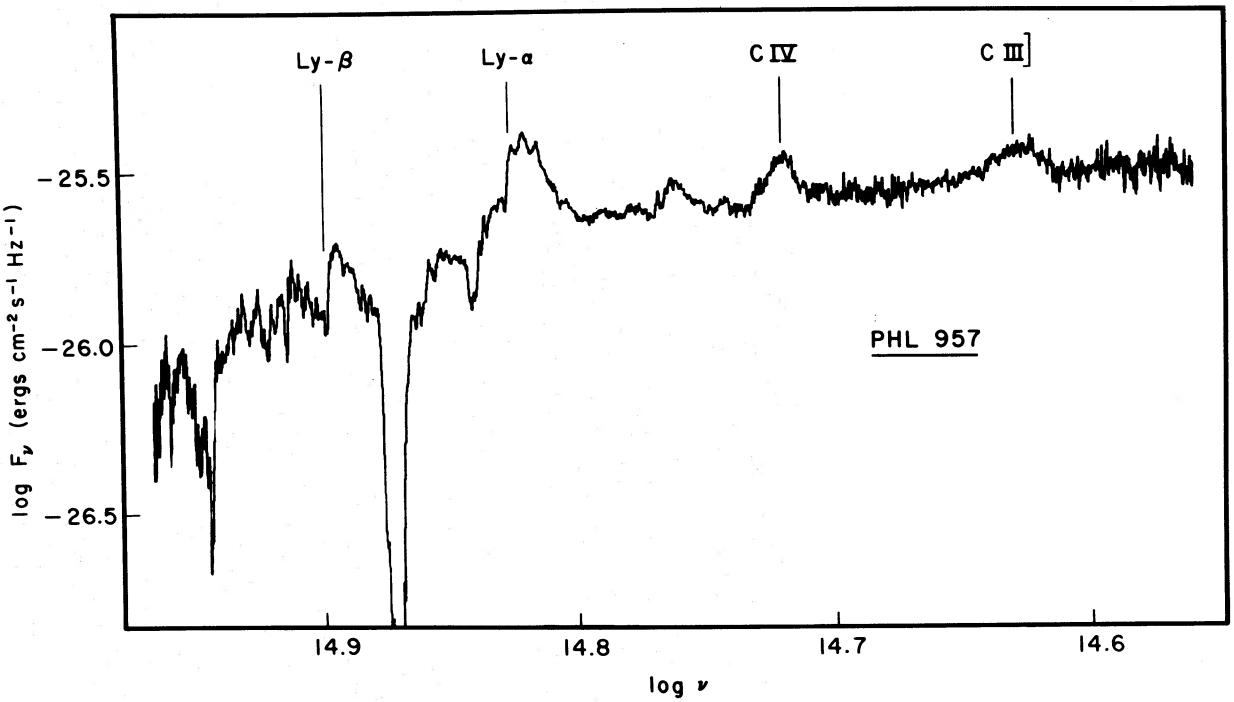

FIG. 1.—Sum of low-resolution Lick scans of PHL 957

The Steward observations were made with the cross-dispersed echelette spectrograph and RCA 33063 image tube at the 2.3 m telescope. This system has been described by Carswell *et al.* (1975), the only subsequent modification of any note being the introduction of a focal-plane mask to suppress image-tube ion events and dark current. Six echelette spectrograms were obtained with exposure times in the range 50^m–90^m depending on conditions; one of these, SI 1525, is reproduced in Figure 2 (Plate 1). The plates were all scanned on the PDS microdensitometer at Kitt Peak National Observatory, using a 16 μ × 16 μ slot size and 8 μ steps. Further reductions were carried out on the CDC 6400 computers at the University of Arizona and the Kitt Peak National Observatory. The spectra were smoothed by convolving with a Gaussian with a full width at half-maximum of four PDS scan steps and then converted to intensity, using a calibration step wedge, and to a common wavelength scale. The individual spectra were then added. The more recent spectra were more heavily weighted to reflect the higher signal-to-noise ratio due to the use of the mask. The actual wavelength scale was determined from plates SI 1525 and 1531, and was not corrected to vacuum or to the Sun. The resulting relative intensity tracings are shown in Figure 3 for orders 8 through 13. The tracing for order 13 is the sum of only three plates, since there was no significant information in that order on the remaining plates. Some indication of the signal-to-noise ratio for an individual spectrogram can be obtained from Figure 4, which presents the relative intensity tracings for order 10 for each plate.

Table 3 lists those lines that appeared to be present on all spectra and were thus deemed "certain"; a total of 203 such lines were found. There are, however, many other weak features that may be real but are not listed. Table 3 also contains an estimate of line strength on a (1–5) scale. We appear to have good-quality coverage from about 3140 Å to about 5600 Å with some lower signal-to-noise information out to about 6400 Å.

A direct comparison shows that many of the lines from the LMZOS low-dispersion image-tube spectra appear to have been blends of two or more closely spaced lines. The correspondence in the ultraviolet

TABLE 2

EMISSION-LINE STRENGTHS

Emission Line	λ (1st Moment)	z	W_λ	FWHM	Flux
Lα λ1216.....	4544	2.737	128	146	119
Si IV λ1400.....	5174	2.696	16	76	13
C IV λ1549.....	5696	2.677	47	129	33
C III] λ1909.....	7030	2.683	68	308	35

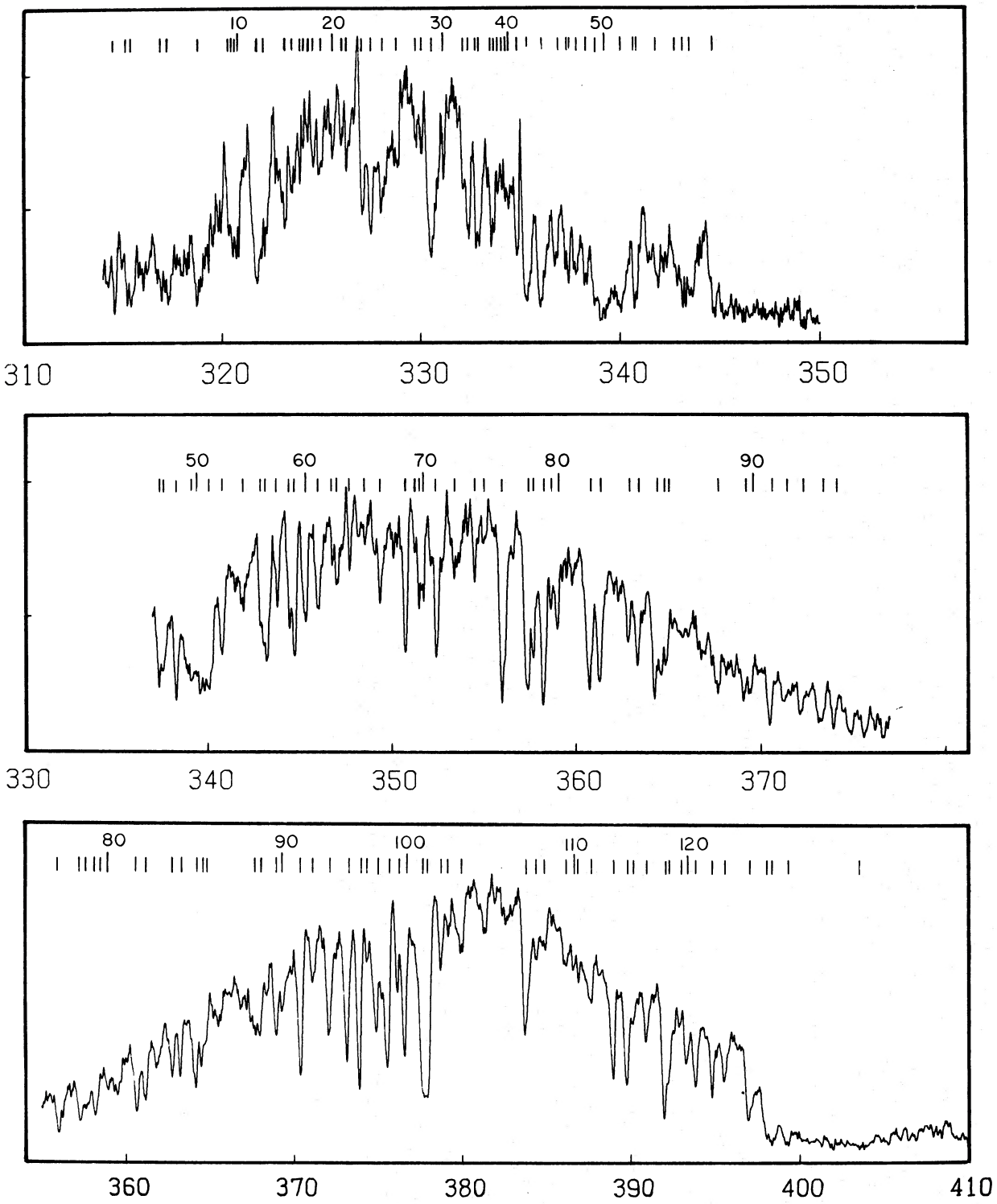

FIG. 3.—Summed relative intensity distributions derived from six echelette spectrograms of PHL 957. Wavelengths are given in nanometers.

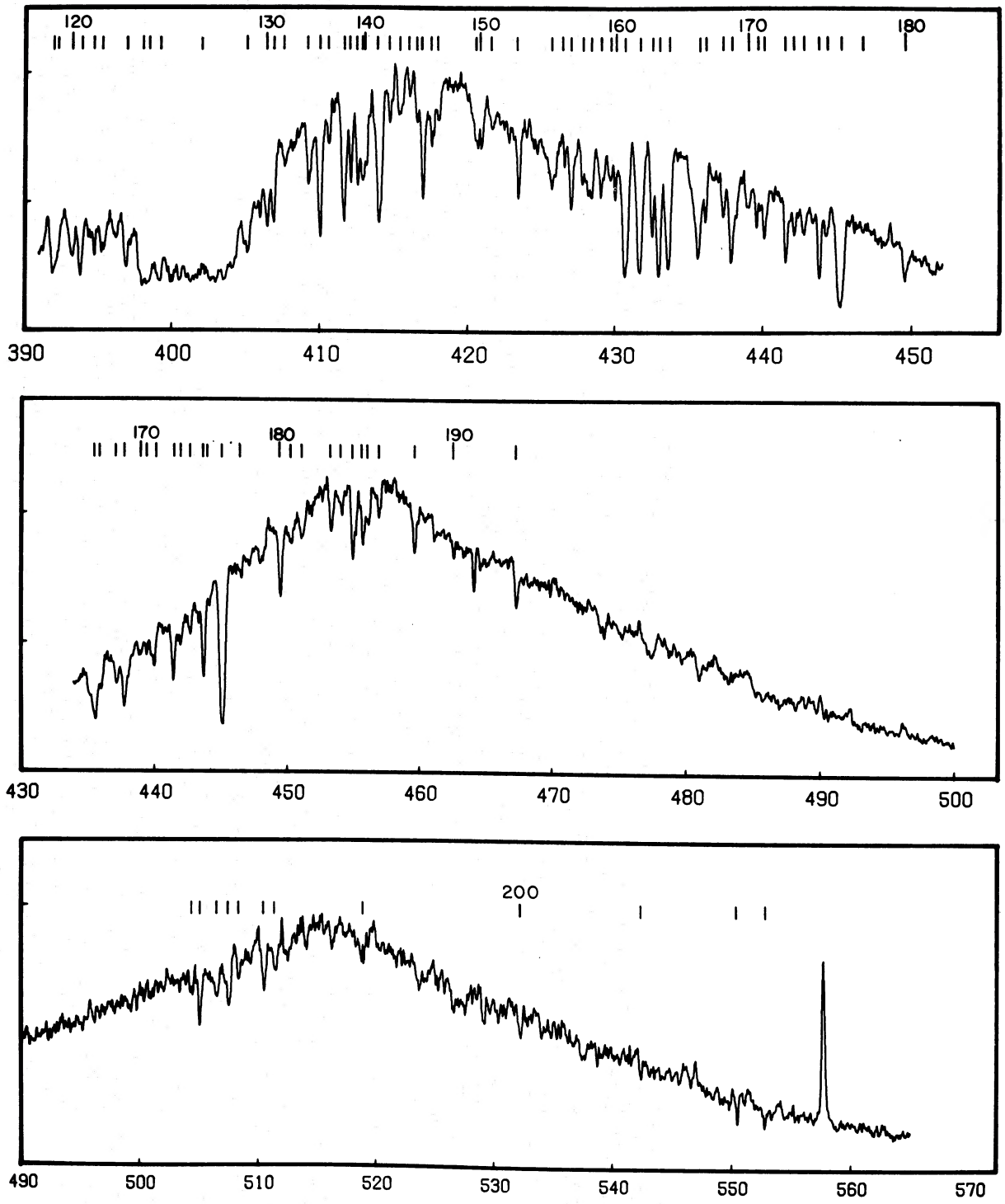

FIG. 3.—*Continued*

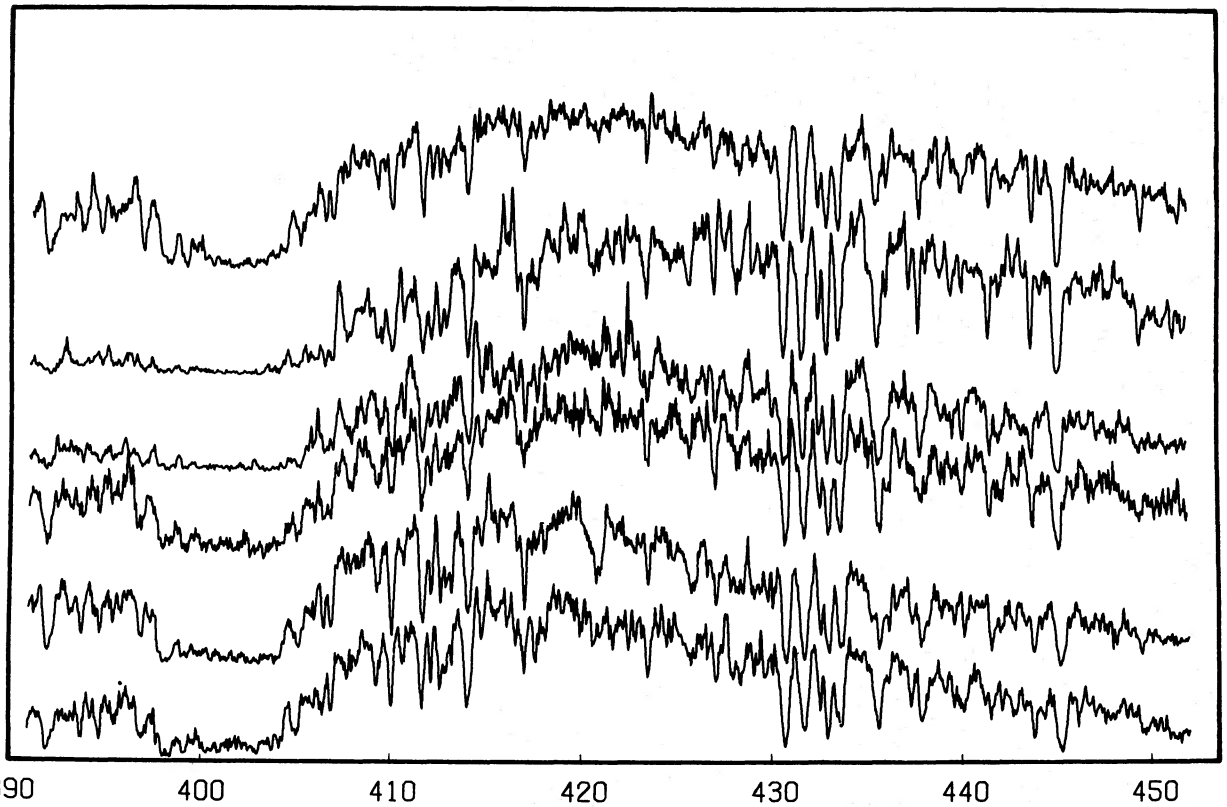

FIG. 4.—Individual relative intensity distributions of the tenth spectrum order as derived from six echelette spectrograms. Wavelengths are in nanometers.

region is good, but longward of emission Lα we have been able to confirm only four of their 10 features. A similar comparison with the LMZOS and Wingert (1975) high-dispersion TV data indicates that some of our lines are likewise blends of unresolved close lines. For example, we are unable in the summed spectra to resolve the two lines at 4305.78 and 4308.06 Å found by LMZOS. Of the remaining 30 lines in the LMZOS TV spectrum, we are unable to find six, all with estimated strengths of $\frac{1}{2}$ or less. It is uncertain whether this is due to our lower resolution, or to noise problems (theirs or ours). Comparison with Wingert's data shows that all of his "certain" lines are confirmed by us except for (*a*) a feature at 3667 Å for which there is some evidence in Figure 3 but which has not been listed in Table 3, (*b*) 12 very close pairs (separation < 2 Å) which we have listed as a single line, and (*c*) the features at 3863 and 3982 Å which we resolve into two lines at 3861–3866 and 3981–3984 Å, respectively. (Both the 3863 and 3982 regions are covered by two of Wingert's scans, but a comparison suggests that the signal-to-noise is rather poor.) We are able to confirm 24 of Wingert's "possible" lines, and a further seven of his close pairs of "possible" lines are seen as at least single features in our data. Five of our lines (3792, 3877, 4180, 4297, and 4460 Å), all strength 1, do not appear in Wingert's list.

III. THE EMISSION SPECTRUM

a) The Continuum

Longward of the Lα emission line the continuum may be fitted rather well with a power-law spectrum of the form $f_\nu \propto \nu^{-0.6\pm0.1}$ ergs cm^{-2} s^{-1} Hz^{-1}. This appears to be in reasonable agreement with the continuum data given by LMZOS. Shortward of Lα, however, the continuum is substantially lower than the level projected from higher wavelengths (see Fig. 1), although it almost reaches the projected value at a point immediately shortward of the strong Lα absorption and close to the expected position of Lβ in the emission system. The continuum deficiency is almost certainly due to the very large number of absorption lines found shortward of Lα; it is a fairly common occurrence in QSOs with very rich absorption spectra.

b) The Emission Lines

Emission-line equivalent widths, full widths at half-maximum, and energy flux are given in Table 2 for the Lα, Si IV λ1397, C IV λ1549, and C III] λ1909 transitions. It is not possible to tell from our data[1] whether or not

[1] We note that because of the blaze characteristics of the echelette system and the use of a photographic detector,

TABLE 3

ABSORPTION LINES IN PHL 957

1	3145.9	1	52	3407.6	2	103	3788.0	1	154	4266.2	1
2	3152.4	1	53	3408.7	1	104	3792.5	1	155	4270.6	2
3	3154.3	1	54	3419.4	2	105	3800.4	1	156	4278.3	1
4	3169.7	1	55	3428.9	2	106	3837.9	3	157	4283.4	1
5	3173.0	1	56	3432.4	3	107	3844.9	1	158	4290.8	1
6	3187.5	2	57	3438.2	1	108	3850.3	1	159	4297.3	1
7	3203.9	1	58	3445.2	1	109	3861.8	1	160	4300.5	1
8	3205.8	2	59	3447.7	3	110	3866.5	1	161	4307.1	4
9	3207.6	2	60	3453.2	2	111	3869.6	1	167	4317.4	4
10	3208.9	1	61	3460.7	2	112	3877.2	1	163	4325.6	2
11	3218.1	3	62	3467.8	1	113	3890.0	3	164	4329.7	4
12	3222.0	1	63	3470.5	2	114	3897.9	3	165	4336.4	4
13	3232.1	2	64	3477.5	2	115	3901.4	1	166	4356.5	3
14	3235.7	1	65	3485.8	1	116	3909.2	2	167	4361.2	1
15	3239.8	1	66	3493.8	2	117	3920.0	3	168	4372.9	1
16	3241.4	1	67	3507.7	3	118	3922.3	1	169	4378.5	3
17	3243.8	1	68	3512.6	1	119	3929.3	1	170	4389.6	1
18	3246.6	1	69	3515.0	1	120	3932.8	2	171	4395.6	1
19	3249.3	1	70	3517.6	1	121	3938.5	2	172	4401.0	2
20	3256.2	1	71	3524.4	3	122	3948.1	2	173	4415.2	2
21	3260.2	1	72	3534.1	1	123	3955.2	2	174	4420.8	1
22	3263.2	1	73	3545.2	2	124	3969.8	3	175	4427.6	1
23	3271.2	2	74	3550.4	1	125	3981.7	2	176	4437.9	3
24	3275.4	2	75	3560.0	4	126	3984.0	2	177	4442.2	1
25	3280.5	2	76	3573.8	4	127	3992.4	2	178	4452.0	5
26	3288.9	1	77	3576.9	3	128	4022	6 vb	179	4466.8	1
27	3298.2	1	78	3582.4	4	129	4051.8	1	180	4495.4	3
28	3301.0	1	79	3586.6	1	130	4065.2	2	181	4503.4	2
29	3305.6	3	80	3590.3	2	131	4069.3	2	182	4511.2	1
30	3312.0	1	81	3607.2	3	132	4077.1	1	183	4533.7	2
31	3321.9	1	82	3612.8	3	133	4093.1	2	184	4541.8	1
32	3324.3	2	83	3628.5	1	134	4100.9	3	185	4550.2	2
33	3328.2	2	84	3633.2	2	135	4107.0	1	186	4557.5	2
34	3329.8	2	85	3642.6	3	136	4117.0	3	187	4561.9	1
35	3335.8	2	86	3645.8	2	137	4121.6	2	188	4569.6	1
36	3337.2	1	87	3648.2	1	138	4126.2	2	189	4596.3	2
37	3339.2	1	88	3675.8	1	139	4129.3	2	190	4626.1	1
38	3341.4	1	89	3690.6	2	140	4132.2	1	191	4673.2	2
39	3342.9	1	90	3694.1	1	141	4140.6	3	192	5044.9	1
40	3344.6	1	91	3704.7	4	142	4148.9	1	193	5051.0	2
41	3348.7	2	92	3712.2	1	143	4156.6	1	194	5065.8	1
42	3353.3	3	93	3721.4	2	144	4161.2	1	195	5075.3	2
43	3360.5	3	94	3732.3	3	145	4166.3	1	196	5083.6	1
44	3367.7	1	95	3739.4	3	146	4170.2	3	197	5105.4	2
45	3373.3	2	96	3744.6	1	147	4176.3	1	198	5114.2	1
46	3374.9	1	97	3749.3	2	148	4180.6	1	199	5189.2	1
47	3379.0	1	98	3755.9	3	149	4207.4	1	200	5323.2	1
48	3382.7	1	99	3762.2	1	150	4209.5	1	201	5424.6	1
49	3388.0	1	100	3766.5	3	151	4216.8	1	202	5505.2	1
50	~3392	4 b	101	3777.0	4	152	4234.8	2	203	5528.2	1
51	3400.5	3	102	3779.9	4	153	4257.6	1			

there is a Lβ emission line. As noted above, the continuum is heavily absorbed below Lα, and the apparent peak of Lβ (shown in Fig. 1) barely reaches the extrapolated continuum level; it could well be caused by an absence of absorption. If there is Lβ emission, its intensity could be as large as half that of Lα without serious disagreement between the redward wings of the profiles of the two lines. The data are quite compatible with the 1 : 5 ratio predicted for recombinations in an optically thin gas (Bahcall 1966). Although both lines seem to be sharply cut off on their short-wavelength sides, as if by Lyman line absorption, the Lα emission maintains strength noticeably further shortward than does the "Lβ emission." This could be due to a narrow Lα emission component at $z = 2.683$ which is partly filling in the Lα absorption trough on the shortward wing of the line, although this interpretation is required only if there actually is Lyman absorption in both areas. It is interesting that $z = 2.683$ is also the redshift of the centroid of the C III] λ1909 line, although its profile seems quite different. The narrow spike on the longward wing of Lα at λ4570 could then be interpreted as N v λ1240 in this redshift system.

The three strongest emission lines Lα, C IV λ1549, and C III] λ1909 all have different profiles. These are shown in Figure 5 reduced to a common redshift. Part of the difference may be due to blending between Lα and N v λ1240, and perhaps between C III] λ1909 and Si III] λ1895 or Al III $\lambda\lambda$1854, 1862. Absorption may also play a role, for example, in the shortward wing of Lα. It is clear, however, that the C IV λ1549 line does not extend nearly as far longward (or indeed shortward, although this could be due to blending) as does C III] λ1909. It is possible that the wings of the C III] line are coming from gas which does not emit

virtually no information on broad emission lines may be derived from the echelette data. The ITS, however, is well suited to this type of work.

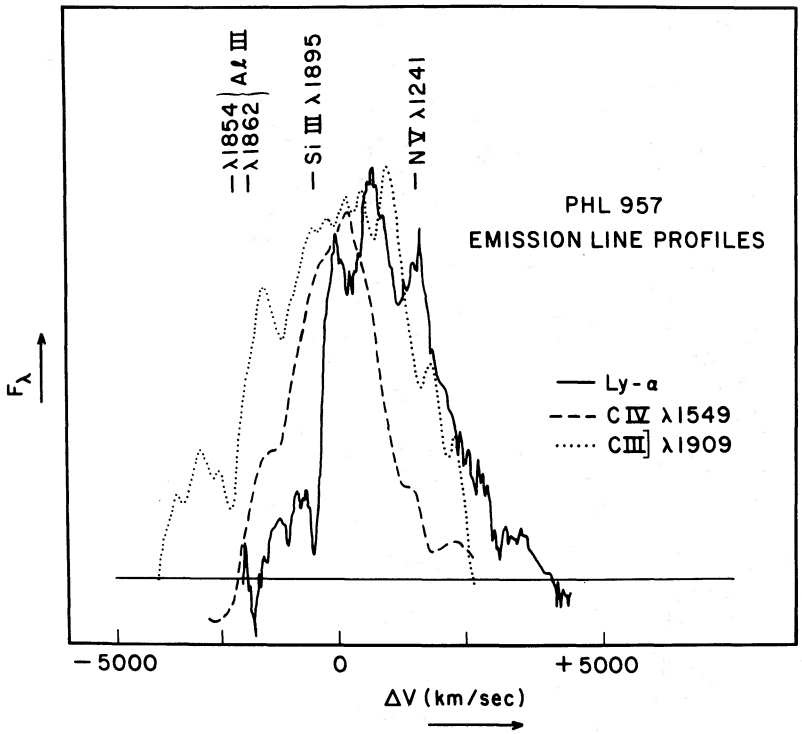

FIG. 5.—Emission-line profiles of Lα, C IV λ1549, and C III] λ1909 reduced to a common redshift $z = 2.68$

C IV λ1549. Alternatively, the relative sharpness of the C IV line could be due to self-absorption, while the C III] line is unaffected because of its low transition probability. Line asymmetries of this type are again fairly common among high-redshift QSOs. Their interpretation almost certainly involves outflow of material from the QSO (cf. Ptak and Stoner 1973; MacAlpine 1974; Blumenthal and Mathews 1975). Indeed, in studying Figure 5, one is led to speculate that the broad features may be made up of several narrower emission components implying discrete emission regions with velocities differing by $\sim 10^3$ km s^{-1}. The difference in profiles leads to uncertainty in the true emission-line redshift of order 1–3 × 10^3 km s^{-1}.

The relative strengths of the Lα, Si IV, C IV, and C III] lines are again fairly similar to other high-redshift QSOs. Similar values have been obtained from a variety of model calculations (see, for example, Davidson 1972) on the assumption of solar composition. These data are thus consistent with a normal distribution of elements. Helium is the only possible exception, since the He II λ1640 line has not been detected either by us or by LMZOS. However, Williams (1971) has shown this is not necessarily inconsistent with a normal helium abundance, but depends, in a photoionization model, on the ratio of He^+ to H ionizing photons. There is some supporting evidence from the absorption lines (see below) that this ratio may be low in PHL 957. Such an explanation would, however, argue against a strong N V contribution to the emission spectrum.

c) *The Absorption Spectrum*

For quasars with rich absorption spectra, the identification of the absorption lines can be both complicated and frustrating. As the number of lines increases, so do both the number of candidate redshifts and the probability of getting an acceptable redshift by chance. In our analysis, we searched for wavelength ratios among the strong lines (lines of strength $\gtrsim 2$) that corresponded to the ratio of selected doublets or other pairs of strong transitions (e.g., Lα, Lβ). We also checked all strong lines as possible Lα lines. In this way we obtained a total of ~200 candidate redshift systems (not all independent) out of only 96 strong lines. Possible identifications of the strength 1 lines within these redshift systems were then sought.

The next step was to reduce the number of candidate redshifts to a manageable set. Our procedure was to determine a probability of identifying the lines in a given redshift system by chance. A formula for calculating the probability of chance coincidence was given by Russell and Bowen (1929). Although recent papers by Havnes and van den Heuvel (1972) and Cowley and Aller (1972) have pointed out some problems in the use of the Russell-Bowen formulae when the density of detected lines is near saturation at the experimental resolution, these objections seem less important in the present application.

The first step in our probability calculations was to divide the observed spectrum into five intervals contain-

ing approximately equal numbers of observed lines. This was done because of the distinctly nonuniform distribution of lines in the spectrum of PHL 957. In common with many other absorption-line QSOs, there is a very noticeable deficiency of absorption lines at wavelengths longer than the Lα emission line. We then determined the probability that a randomly chosen wavelength in each of these intervals would fall within ϵ of an observed line, by taking the ratio of the total wavelength interval within ϵ of the observed lines divided by the total wavelength range of the interval. This empirical value for p, the probability of identifying a single randomly chosen line with one of the observed lines, was normally slightly larger than the theoretical value derived by Russell and Bowen. We then found the number M_i of transitions that would occur in each of the i intervals at the given redshift. The probability of identifying J lines at the redshift z is then

$$P(J, z) = \sum \left\{ \pi_i \left[\frac{M_i!}{(M_i - j_i)! j_i!} p_i^{j_i} (1 - p_i)^{M_i - j_i} \right] \right\}$$

where the sum is made over all j_i subject to the constraints that

$$\sum j_i = J$$

and

$$j_i \leq \min (N_i, M_i) .$$

The probability of identifying J or more lines is then an "index of reality" and can be used to eliminate a large fraction of the candidate redshift systems.

A total of 16 systems were found to have a probability less than 10^{-2} of occurring by chance. Four other systems were included for further analysis because they had been identified in earlier analyses. We do not, of course, wish to imply that none of the remaining systems is real. For example, some of the Lα–Lβ pairs may be genuine (see discussion below), but there does not seem to be any way of demonstrating this for an individual case. We should emphasize that this procedure is viewed as a simple, computationally inexpensive first look at the data. Questions of relative line strength, ionization distributions, etc., are analyzed subsequently by inspection.

In Table 4 we list the final set of 20 redshift systems analyzed using these procedures. An indication of our confidence in the reality of each system, based on the above index, is likewise given. Systems *A* through *J* are those suggested by LMZOS. Table 5 presents possible line identifications in the five most probable systems. The oscillator strengths listed in Table 5 have been obtained from Wiese, Smith, and Glennon (1966), Wiese, Smith, and Miles (1969), and Morton and Smith (1973). Excited fine-structure lines are also listed in those cases where the identifications seem possible. Four redshift systems found by LMZOS are classified as doubtful because of (*a*) the high probability of the identification occurring by chance, and (*b*) unsatisfactory ionization and line strength characteristics. A reanalysis of the LMZOS data led Bahcall and Joss (1973) to reject five of the 10 LMZOS redshift systems, including four systems that we have listed as possible. Three of the five systems that Bahcall and Joss confirmed have been rejected by our procedure. While it is uncertain whether these differing results are caused by the differences in procedure or in observational data, we were able to reject only one of the final 20 systems that we studied by application of the technique discussed by Bahcall (1968). In general, there were so many suggested identifications that it was possible to reject enough lines to give a reasonable ionization structure while still satisfying Bahcall's remaining criteria.

Since so much attention has recently been focused on the existence of closely split pairs of redshift systems, we wish to emphasize that neither of the two

TABLE 4

POSSIBLE REDSHIFT SYSTEMS

System	z	P	Comment
A	2.3088	6×10^{-5}	V. Strong Lα, cf. 1331+170 systems *A*, *B*
B	2.6624	2×10^{-3}	
C	2.2050	3×10^{-2}	
D	2.2250	3×10^{-1}	Doubtful
E	2.0708	8×10^{-1}	Doubtful
F	2.5513	1×10^{-1}	Doubtful
G	2.5433	1×10^{-1}	Doubtful
H	2.1061	1×10^{-2}	
I	1.8234	2×10^{-2}	
J	2.1565	7×10^{-3}	
K	1.7969	1×10^{-4}	cf. 1331+170 system *C*
L	2.6187	5×10^{-4}	Lα rather weak
M	1.7188	2×10^{-3}	All lines weak except Lα
N	1.5535	2×10^{-2}	Low ionization
O	2.2759	2×10^{-2}	Wide ionization range, not self-consistent
P	2.2747	2×10^{-2}	
Q	0.4242	2×10^{-2}	Fe II > Mg II
R	1.7348	4×10^{-2}	Line strengths inconsistent
S	0.5037	9×10^{-2}	No Mg II
T	1.9888	1×10^{-1}	Doubtful

TABLE 5

IDENTIFICATIONS IN FIVE PROBABLE REDSHIFT SYSTEMS

System A <z> = 2.3088

Line	λ	S	ID		F	z	Δλ	Comments[+]
11	3218.1	3	Ly-γ	972.5	.029	2.3091	.3	
13	3232.1	2	CIII	977.0	.674	2.3082	-.6	
23	3271.2	2	OI	988.8		2.3083	-.5	
24	3275.4	2	NIII	989.8	.107	2.3092	.4	
			SiII	989.9	.244	2.3088	.0	
41	3348.7	2	SIII	1012.5		2.3074	-1.4	
47	3379.0	1	SiII	1020.7	.048	2.3105	1.7	M, B
50	∿3392	4 b	Ly-β	1025.7	.079	2.3070	---	L, B
55	3428.9	2	CII	1036.3	.125	2.3088	.0	M
62	3467.8	1	AII	1048.2	.230	2.3083	-.5	
69	3515.0	1	SIV	1062.7	.038	2.3076	-1.3	
79	3586.6	1	NII	1084.0	.101	2.3087	-.1	
98	3755.9	3	NI	1134.6	∿.05	2.31033	1.7	L, B
103	3788.0	1	FeII	1144.9		2.3086	-.2	M
113	3890.3	3	CIII*	1175.6		2.3090	.2	
121	3938.5	2	SIII	1190.2	.022	2.3091	.4	
			SiII	1190.4	.650	2.3086	-.3	
122	3948.1	2	SiII	1193.3	1.300	2.3086	-.3	
124	3969.8	3	NI	1199.9	.133	2.3084	-.4	B
127	3992.4	2	SiIII	1206.5	1.660	2.3091	.3	
128	∿4022	6 vb	Ly-α	1215.7	.416	2.3084	---	
141	4140.6	3	SII	1250.6	.005	2.3109	2.6	Δλ large, too strong
142	4148.9	1	SII	1253.8	.011	2.3091	.3	M
145	4166.3	1	SII	1259.5	.016	2.3079	-1.1	
146	4170.2	3	SiII	1260.4	.959	2.3086	-.2	
161	4307.1	4	OI	1302.2	.049	2.3076	-1.6	L, B, too strong
162	4317.1	4	SiII	1304.4	.147	2.3096	1.1	L, too strong
173	4415.2	2	CII	1334.5	.118	2.3085	-.4	
193	5051.0	2	SiII	1526.7	.076	2.3084	-.5	
200	5323.2	1	FeII	1608.4		2.3096	1.3	
203	5528.2	1	AIII	1670.8	1.880	2.3087	-.1	
Possible Excited Fine Structure Lines								
25	3280.5	2	NIII	991.6		2.3083	-.5	M
49	3388.0	1	SiII	1023.7		2.3096	.8	
51	3400.5	3	OI	1027.4		2.3098	1.1	K
56	3432.4	3	CII	1037.0		2.3099	1.2	
80	3590.3	2	NII	1084.6		2.3102	1.6	
			NII	1085.7		2.3069	-2.0	
174	4420.8	1	CII	1335.7		2.3097	1.3	B
195	5075.3	2	SiII	1533.4		2.3098	1.7	L

System K <z> = 1.7969

Line	λ	S	ID		f	z	Δλ	Comments
5	3173.0	1	NI	1134.6		1.7966	-.3	
7	3203.9	1	FeII	1144.9		1.7984	1.8	
26	3288.9	1	CIII*	1175.6		1.7976	.9	
33	3328.2	2	SIII	1190.2		1.7963	-.6	L
34	3329.8	2	SiII	1190.4	.650	1.7972	.4	Too strong
36	3337.2	1	SiII	1193.3	1.300	1.7966	-.3	
42	3353.3	3	NI	1199.9	.133	1.7946	-2.6	L, Δλ large
46	3374.9	1	SiIII	1206.5	1.660	1.7973	.5	
51	3400.5	3	Ly-α	1215.7	.416	1.7972	.4	A-f
67	3507.7	3	SII	1253.8		1.7977	1.0	
71	3524.4	3	SII	1259.5		1.7982	1.8	
			SiII	1260.4	.959	1.7963	-.8	
85	3642.6	3	OI	1302.2	.049	1.7973	.5	
87	3648.6	1	SiII	1304.4	.147	1.7968	.0	
94	3732.3	3	CII	1334.5	.118	1.7968	-.1	L
114	3897.9	3	SiIV	1393.8	.528	1.7966	-.4	
118	3922.3	1	SiIV	1402.8	.262	1.7960	-1.1	L
155	4270.6	2	SiII	1526.7	.076	1.7973	.6	Too strong
164	4329.7	4	CIV	1548.2	.194	1.7966	-.4	
165	4336.4	4	CIV	1550.8	.097	1.7962	-1.0	
191	4673.2	2	AlII	1670.8	1.880	1.7970	.2	
199	5189.2	1	AlIII	1854.7	.539	1.7979	1.9	
Possible Excited Fine Structure Lines								
38	3341.4	1	SiII	1194.5		1.7973	.5	L
41	3348.7	2	SiII	1197.4		1.7966	.3	A
72	3534.1	1	SiII	1264.7		1.7944	-3.1	L, Δλ very large
158	4290.8	1	SiII	1533.4		1.7982	2.1	Δλ large
196	5083.6	1	SiII	1816.9		1.7980	2.0	Δλ large

TABLE 5—Continued

System L <z> = 2.6187

Line	λ	S	ID		f	z	Δλ	Comments
23	3271.2	2	CII	904.0		2.6186	-.1	
30	3312.0	1	NII	915.6	.149	2.6173	-1.3	B
33	3328.2	2	AII	919.8	.009	2.6184	-.3	K
38	3341.4	1	Ly-8	923.1		2.6198	1.0	K-f
42	3353.3	3	Ly-7	926.2		2.6205	1.7	K, B, too strong
44	3367.7	1	Ly-6	930.7		2.6185	-.2	M, B
50	~3392	4 b	Ly-ε	937.8	.008	2.6170	-1.6	A, B, too strong
57	3438.2	1	Ly-δ	949.7	.014	2.6203	1.5	M-f
70	3517.6	1	Ly-γ	972.5	.029	2.6171	-1.6	
72	3534.1	1	CIII	977.0	.674	2.6173	-1.4	K-f
77	3576.9	3	OI	988.8		2.6174	-1.3	B
78	3582.4	4	NIII	989.8	.107	2.6193	.6	
			SiII	989.9	.244	2.6190	.3	
90	3694.1	1	SiII	1020.7	.048	2.6192	.5	
92	3712.2	1	Ly-β	1025.7	.079	2.6192	.5	
94	3732.2	3	OVI	1031.9	.130	2.6169	-1.8	K
97	3749.3	2	CII	1036.3	.125	2.6180	-.7	
98	3755.9	3	OVI	1037.6	.065	2.6198	1.2	A, B
104	3792.5	1	AI	1048.2	.230	2.6181	-.6	B
109	3861.8	1	AI	1066.7	.059	2.6203	1.8	
118	3922.3	1	NII	1084.0	.101	2.6184	-.4	K
135	4107.0	1	NI	1134.6		2.6198	1.2	
161	4307.1	4	SiII	1190.4	.650	2.6182	-.6	A, B, too strong
162	4317.1	4	SiII	1193.3	1.300	2.6178	-1.1	A
172	4401.0	2	Ly-α	1215.7	.416	2.6201	-1.9	
187	4561.9	1	SiII	1260.4	.959	2.6194	.9	
192	5044.9	1	SiIV	1393.8	.528	2.6195	1.2	M
195	5075.3	2	SiIV	1402.8	.262	2.6180	-1.0	A-f, too strong

System B <z> = 2.6624

Line	λ	S	ID		f	z	Δλ	Comments
30	3312.0	1	CII	904.0		2.6637	1.2	L
42	3353.3	3	NII	915.6	.149	2.6624	.0	K, L
44	3367.7	1	AII	919.8	.009	2.6613	-1.0	L, M
47	3379.0	1	Ly-8	923.1		2.6605	-1.7	M, A
50	~3392	4 b	Ly-7	926.7		2.6623	-.1	A, L, too strong
52	3407.6	2	Ly-6	930.7		2.6613	-1.0	
56	3432.4	3	Ly-ε	937.8	.008	2.6601	-2.2	A-f, Δλ large
64	3477.5	2	Ly-δ	949.7	.014	2.6617	-1.7	
75	3560.5	4	Ly-γ	972.5	.029	2.6607	-1.2	
77	3576.9	3	CIII	977.0	.674	2.6611	-1.2	L
95	3739.4	3	SiII	1020.7	.048	2.6636	1.2	Too strong
98	3755.9	3	Ly-β	1025.7	.079	2.6618	-.6	A, L
102	3779.9	4	OVI	1031.9	.130	2.6630	-.7	
104	3792.5	1	CII	1036.3	.125	2.6596	-2.8	L, Δλ too large
105	3800.4	1	OVI	1037.6	.065	2.6627	.3	
106	3837.9	3	AI	1048.2	.230	2.6614	-1.0	
124	3969.8	3	NII	1084.0	.101	2.6622	-.2	A
143	4156.6	1	NI	1134.6		2.6635	1.3	
161	4307.1	4	CIII*	1175.6		2.6638	1.6	A, L
167	4361.2	1	SiII	1190.4	.650	2.6636	1.5	
168	4372.9	1	SiII	1193.3	1.300	2.6645	2.6	M, Δλ large
171	4395.6	1	NI	1199.9	.133	2.6633	1.1	
174	4420.8	1	SiIII	1206.5	1.660	2.6642	2.1	A-f, Δλ large
178	4452.0	5	Ly-α	1215.7	.416	2.6621	-.4	
197	5105.4	2	SiIV	1393.8	.528	2.6629	.8	

System M <z> = 1.7188

14	3235.7	1	SiII	1190.4	.650	1.7182	-.8	
17	3243.8	1	SiII	1193.3	1.300	1.7183	-.6	
22	3263.2	1	NI	1199.9	.133	1.7196	.9	
25	3280.5	2	SiIII	1206.5	1.660	1.7190	.2	A-f
29	3305.6	3	Ly-α	1215.7	.416	1.7191	.3	
44	3367.7	1	NV	1238.8	.152	1.7185	-.4	B, L
47	3379.0	1	NV	1242.8	.076	1.7189	.0	A, B

TABLE 5—Continued

System M <z> = 1.7188 (continued)								
Line	λ	S	ID		f	z	Δλ	Comments
55	3428.9	2	SiII	1260.4	.959	1.7205	2.1	A
73	3545.2	2	SiII	1304.4	.147	1.7179	-.9	
83	3628.5	1	CII	1334.5	.118	1.7190	.2	
103	3788.0	1	SiIV	1393.8	.528	1.7178	-1.5	A
142	4148.9	1	SiII	1526.7	.076	1.7176	-1.9	A
150	4209.5	1	CIV	1548.2	.194	1.7190	.2	
151	4216.8	1	CIV	1550.8	.097	1.7191	.4	
168	4372.9	1	FeII	1608.4		1.7188	-.1	
184	4541.8	1	AlII	1670.8	1.880	1.7183	-.8	
192	5044.9	1	AlIII	1854.7	.539	1.7201	2.3	L
194	5065.8	1	AlIII	1862.8	.268	1.7194	1.2	
Possible Excited Fine Structure Lines								
18	3246.6	1	SiII	1194.5		1.7180	-1.1	
20	3256.2	1	SiII	1197.4		1.7194	.7	
57	3438.2	1	SiII	1264.7		1.7186	-.3	L
75	3560.0	4	SiII	1309.3		1.7190	.2	
84	3633.2	2	CII	1335.7		1.7201	1.6	
146	4170.2	3	SiII	1533.4		1.7196	1.1	

+Capital letters in the last column denote other systems to which the line has been ascribed. An additional f denotes a possible fine structure level.

redshift systems at 2.27 is considered well established. Higher resolution studies will be required before the existence of this pair of systems can be confirmed or rejected.

d) Search for Lα–Lβ Pairs

A striking and characteristic feature of the spectra of absorption-line–rich QSOs is the comparative dearth of lines longward of Lα emission. For example, in PHL 957 the number density (A^{-1}) of detected lines in this spectral region is an order of magnitude less than at shorter wavelengths. This property led Lynds (1971) to suggest that most of the absorption lines were due to Lα. In an attempt to check this hypothesis for PHL 957 we have searched for Lα–Lβ pairs over the entire spectral range; the ratio of line strengths should always be less than ~ 5. The wavelength range was divided into 10 intervals containing equal numbers of lines (except the last). For each Lα candidate a search was

TABLE 6

SEARCH FOR Lα–Lβ PAIRS

λ_l	z_l	N	N_α	N_β	P	N_{exp}	ΔN	Prob	N_γ
Case 1: $\epsilon = 1$, all lines retained									
3130.....	2.052	20	17	6	0.30	5.1	0.9	0.40	...
3258.....	2.177	20	15	5	0.43	6.5	−1.5	0.85	...
3346.....	2.263	20	10	6	0.35	3.5	2.5	0.096	2
3456.....	2.370	20	20	9	0.28	5.6	3.4	0.082	5
3598.....	2.509	20	26	9	0.23	6.0	3.0	0.12	4
3771.....	2.677	20	11	4	0.24	2.7	1.3	0.27	2
3935.....	2.837	20	1	0	0.20	0.2	−0.2	1.0	0
4136.....	3.033	20	5	1	0.24	1.2	−0.2	0.74	0
4303.....	3.196	20	4	2	0.20	0.8	1.2	0.19	0
4499.....	3.387	23	3	0	0.02	0.1	−0.1	1.0	0
Case 2: $\epsilon = 1 - S \geq 2$, systems *A* and *K* removed									
3130.....	2.052	15	7	2	0.23	1.6	0.4	0.51	...
3252.....	2.171	15	4	1	0.29	1.2	−0.2	0.75	...
3352.....	2.269	15	7	4	0.24	1.7	2.3	0.061	1
3474.....	2.387	15	4	2	0.20	0.8	1.2	0.19	0
3620.....	2.530	15	5	3	0.19	1.0	2.0	0.050	2
3778.....	2.684	15	5	3	0.18	0.9	2.1	0.045	2
3944.....	2.845	15	0	0	0.15	0.0	0.0	1.0	0
4144.....	3.041	15	2	0	0.18	0.4	−0.4	1.0	0
4699.....	3.387	18	0	0	0.015	0.0	0.0	1.0	0

made for a corresponding Lβ within a wavelength error ϵ. The number of successes per interval was then compared with the number expected by chance based on the probabilities derived as in § III*c*. This analysis was carried out under a number of different conditions on ϵ, Lα strength, and line samples. The basic results, however, did not change dramatically, so we confine ourselves to the two examples listed in Table 6. Both are for $\epsilon = 1$, but no further restrictions were introduced for case 1. For case 2, Lα line strengths were restricted to $S \geq 2$, and all lines identified in system *A* or *K* were first removed. The columns contain (i) the lower wavelength boundary of the interval, λ_l; (ii) the Lβ redshift corresponding thereto, z_l; (iii) the number of lines N in the interval; (iv) the number of Lα candidates N_α; (v) the number of Lβ successes, N_β; (vi) the probability index p; (vii) the expected number of Lβ successes, $N_{\rm exp}$; (viii) $\Delta N = N_\beta - N_{\rm exp}$; (ix) the probability of obtaining the observed number of successes (or greater) if the lines are randomly distributed; and (x) the number of Lγ successes N_γ. The results suggest that around the emission redshift (both sides) there is indeed some excess of Lα–Lβ pairs. There is also some evidence of a second excess around the system *A* redshift. In the more restricted case 2, approximately twice as many pairs (15) were found than were expected on the basis of chance; these are concentrated between the emission and system *A* redshifts. Part of this excess (7.5), however, is already accounted for by some of the redshift systems listed in Table 4. A search was also made for Lγ corresponding to apparent Lα–Lβ pairs for those redshifts at which the line would still be observable. The results in Table 6 again provide some evidence for a slight excess of such identifications at redshifts between $z_{\rm em}$ and z_A. The number of systems in which the optical depth in neutral hydrogen is sufficiently great that Lβ and higher Lyman series lines are detectable, is therefore small, compared with the number of candidate Lα lines. This conclusion is apparently at variance with that of Wingert (1975), who claims 19 Lβ "successes" out of 21 candidate Lα lines in the region covered by his data using a wavelength error of ±1 Å apparently in *both* lines (this corresponds to $\epsilon \pm 2$ Å in our method). We confirm only eight of his systems using $\epsilon = 1$, although we note that three of Wingert's pairs would be members of closely split redshift systems and would not be resolved by us. On two occasions, Wingert uses the same observed feature as Lβ, and all but one of the remaining Wingert pairs have Lβ associated with features of lesser certainty. The discrepancy between our results and Wingert's is thus not as great as appears at first sight. Both analyses thus indicate that if most of the remaining lines are due to Lα as suggested by Lynds, the Lβ lines must be substantially weaker. This would be possible if the optical depth $\tau_{L\alpha}$ of the Lα candidates were of order unity and would, of course, account for the absence of other identifications. Some physical mechanism is, however, presumably required to account for this selection in favor of low Lα optical depth. Such a mechanism has in fact been suggested by Williams (1972), who pointed out that if resonance-line photons are created by collisions in an optically thick cloud, the resultant buildup in line radiation pressure causes the cloud to expand. Near a QSO where a cloud would be heated by incident radiation this mechanism may thus operate to prevent a buildup of optical depth in any one line. If Lα is the first line to go optically thick, this would be the only observable line. If, on the other hand, the energy input were inadequate (for example, if the cloud were shielded from ionizing radiation), large column densities could build up. The ionization state and column density of system *A* could, for example, be understood in these terms. In any event, some mechanism is required to limit the column densities in QSO absorption clouds if the Lα interpretation of the absorption line excess shortward of Lα emission is to be retained. In this context we note an alternative, intrinsic, explanation of the Lα absorption features given by Arons (1972). He suggests that the absorption arises in low mass "protogalaxies" which are kept ionized by radiation from QSOs. In the neighborhood of Lα our data are consistent with his results at least within the rather wide range permitted by uncertainties in the analysis. On the other hand, this type of model implies that the number density of unidentified lines shortward of, say, 3600 Å should be essentially zero as in QSOs with $z_{\rm em} \sim 2$. This is not consistent with our data and seems to be a general objection to this type of explanation of the line densities in high-z QSOs.

IV. DISCUSSION OF INDIVIDUAL ABSORPTION SYSTEMS

a) System A, z = 2.309

The existence of this system seemed well established in previous investigations. We have identified absorption lines with transitions of H, C II, C III, N I, N II, N III, O I, Al II, Si II, Si III, S II, S III, S IV, Ar I, and Fe II. For H I region species the internal consistency of this system is remarkable. The only "missing" low ionization transition was the Ar I λ1066.7 line. Since the transition at 1048.2 Å is identified with a weak line and the oscillator strength is 4 times as large as that of the 1066.7 Å transition, this absence is not surprising. The transitions of higher ionization stages such as C IV, N V, and O VI do not appear to be present, although there may be some weak evidence of features corresponding to the Si IV doublet at 4612 and 4641 Å. (The strength of the feature at 4641 Å is strongly influenced by what may be a dust particle on the image-tube mask for one of the spectra. On this spectrum the "line" reached zero intensity, while on the remaining spectra there was only a suggestion of a line.)

Our identification of lines of C III, N II, N III, Si III, S III, and S IV requires comment in that it appears to be inconsistent with the pure H I cloud model suggested by Beaver *et al.* (1972) and Grewing and Strittmatter (1973). In some cases the identification rests on one or two lines only and is thus doubtful. In particular, the line at 3275.4 Å may be entirely due to Si II λ989.9, with no contribution from the N III line. The small

wavelength discrepancies for the Si III and C III lines argue against their being misidentifications. On the other hand, it is difficult to understand how the C III λ1175 identification can be real since this arises from the metastable $^3P^o$ $2p$ level and, as discussed below, there appears to be little significant population of the excited fine-structure levels of the ground state in Si II or C II. According to Osterbrock (1970), densities greater than $\sim 10^{10}$ cm^3 are required to maintain comparable populations in the ground (^1S) and metastable (^3P) states of C III. The argument is not entirely conclusive, however, since the C III lines could arise in a different region of a cloud moving with the same velocity as the H I region. Some support for the presence of H II region lines comes from the tentative identifications of all the available ground-state lines of S II, S III, and S IV. Even here, however, there are problems since (i) the wavelength agreement is generally poor, (ii) the S III 1190.2 line is also identified with Si II 1190.4, and (iii) given the ratio of Si II/S II and Si II/Si IV it is hard to understand how the S IV lines could appear so strong. The sulfur identifications thus appear doubtful. Thus, while there may well be higher ionization states present than would be expected in a pure H I region, the data do not permit a definite conclusion on this point. The ionization mechanism appears to be limited, however, to energies less than 35–40 eV, perhaps due to shielding from underlying clouds at different redshift.

We have attempted to identify lines from excited fine-structure levels of the ground state since these lines can provide a valuable probe of the physical conditions in the absorbing region (Bahcall and Wolf 1968). Those lines for which the individual wavelength agreement is satisfactory are listed in Table 5. None of these identifications is convincing. Clearly, the fine-structure population in PHL 957 system *A* is small. Since the C II fine-structure level is expected to be more populated than other species, our result is consistent with the tentative identification of the weak feature at λ4419 in the high-resolution LMZOS scan as C II λ1335.

The strong Lyman line absorption in the spectrum of PHL 957 also requires further comment. Beaver *et al.* (1972) showed that the Lα feature at ~4020 Å was consistent in profile with that expected from a column density of neutral hydrogen $N_H \sim 10^{21}$ cm^{-2}. On the other hand, the feature could be produced by a lower value of N_H if the velocity dispersion were high. In order to check this possibility, we have made observations of the Lβ profile using the ITS system at a resolution of ~3.8 Å. Radiation damping profiles for several different column densities were convolved with the instrumental profile and then compared with the observed Lα profile which gave the best fit in the wings. The H^0 column density was $\log N_H \sim 20.88 \pm 0.15$ cm^{-2}. A "predicted" Lβ profile was then computed using this value of N_H and was compared with the observed feature. Unfortunately the comparison at Lβ is rather more difficult because of the very large amount of absorption at this wavelength due to other features. The predicted profile lay above the observed value at all wavelengths so that no inconsistency exists between the observed and predicted Lβ profiles. Although some special form of velocity distribution could be invoked to account for the observations, we consider the high-column-density explanation to be the most plausible in view of (*a*) the sharpness of the metal lines in this system (Morton and Morton 1973) and (*b*) the natural fit of the radiation Lα damping wings to the observations. In view of the similarity between this absorption system and the interstellar absorption spectra observed from the *Copernicus* satellite, we have searched for absorption arising from H_2 (cf. Spitzer *et al.* 1973). No such features were found. This confirms Wingert's (1975) result and is at variance with earlier claims.

The metal to hydrogen abundance in the cloud giving rise to system *A* is also of interest. According to Morton and Morton (1973) the column density in C II is $\sim 10^{14-15}$, which, together with the observed ionization distribution and N_H, implies a C/H $\sim 10^{-5}$ to 10^{-6} (Beaver *et al.* 1972). This is approximately two orders of magnitude below the solar values. The C II lines (λ1036 and λ1334) appear to be strong and approximately equal in our spectra (we estimate equivalent widths $W_{1036} = 0.7 \pm 0.2$ Å, and $W_{1334} = 1.0 \pm 0.2$ Å). The range of possible C II column densities permitted by our data is thus large. A curve-of-growth analysis of the Si II lines is, in principle, possible and could settle the question. There seems, however, to be some uncertainty in the Si II oscillator strengths (Williams *et al.* 1975). The relative strengths of the Si II lines suggest that they are strongly saturated, and they may arise from column densities as high as 10^{17}. We do not, therefore, feel that a markedly anomalous metal to hydrogen abundance has yet been established for system *A*.

Finally we should note the similarity in Lα strength, ionization, and relative velocity with respect to the emission-line system between this system and the line-locked systems *A* and *B* in 1331+170 (Carswell *et al.* 1975).

b) System K, z = 1.797

Our probability estimates suggest that this system is almost as likely to be "real" as system *A*. It is, however, characterized by higher ionization. The C IV and Si IV doublets are strong, but N V has not been detected. This suggests that the He II continuum may be optically thick at the distance of the cloud giving rise to system *K*. Lower ionization species are, however, present, Si II in particular being well established. A search for lines arising from excited fine-structure levels of the ground state may have been successful, several identifications with Si II proving possible. The wavelength agreement is, however, poor, especially in the case of Si II λ1264.7, and the presence of significant Si II fine-structure level population cannot therefore be considered established. We again note the "possible" identification with the C III λ1175 line.

System *K* in PHL 957 seems to be rather similar to system *C* in 1331+170 (Carswell *et al.* 1975) both in

ionization and in velocity relative to the emission system.

c) System B, z = 2.66238

This system was first noted by LMZOS and has subsequently been shown by Wingert (1975) to be double with a splitting ~ 140 km s^{-1}. This splitting may be partially responsible for the rather poor wavelength agreement among the various lines. No feature corresponding to Si II λ1260 was found, leading us to reject other Si II identifications. Similar remarks hold for the C II λ1334 line. The O VI identification is odd if N V is absent. The credibility of the system thus rests primarily on the Lyman lines, especially in view of the splitting found by Wingert.

d) System L, z = 2.618

This system was discussed by Bahcall, Joss, and Cohen (1972) as a possible high-ionization cloud and should, according to our simple probability test, be "real." While a large number of lines have been identified, the errors are large and the internal physical consistency is poor. Thus C II λ1036 is identified, but not C II λ1334; Si II λ1260 is associated with a weak line while Si II λλ989, 1190, and 1193 are identified with strong features; O VI is found, but N V is absent.[2] If the system has physical significance, it rests primarily in the Lyman line identifications.

e) System M, z = 1.71883

This high Δz system again shows a wide range of ionization and, apart from the Lα line, consists mainly of weak features. Except possibly for the absence of Si IV λ1402.8, the system is physically self-consistent.

f) Other Systems

None of the remaining systems seem especially convincing, and no detailed discussion of them will be given. Some comment is, however, required on the higher probability assigned to some of these systems by previous investigators. Virtually all lines listed by LMZOS have been found by us. The problem has been that among our new lines rather few could be ascribed to the previously suggested systems. The plausibility of these is accordingly much reduced. As noted in the previous section, it appears that the great majority of lines detected at wavelengths shortward of the Lα emission arise from multiple clouds with modest ($N_H \sim 10^{14}$ cm^{-2}) neutral-hydrogen column densities. The number of such clouds in the line of sight to PHL 957 is thus of order 10^2, presumably associated with the QSO itself.

g) Line Locking—A Comparison with 1331+170

As noted above, there are many similarities between systems *A* and *K* in PHL 957 and the spectrum of 1331+170 (Carswell *et al.* 1975). These QSOs are the only ones presently known to have very strong Lα absorption profiles, and it is interesting that the redshift displacement factors $D = (1 + z_{em})/(1 + z_{abs})$ are approximately the same (~ 1.11) in both objects. This corresponds to the wavelength ratio of Lβ to the Lyman continuum. In both objects there is a further high probability system (*K* in PHL 957; *C* in 1331+170) in which *D* (~ 1.33) corresponds to the wavelength ratio of Lα to the Lyman continuum. The similarity of redshift factors for the two most probable redshift systems in each QSO is remarkable. This similarity extends to ionization structure also. For example, systems *A* in PHL 957 and *B* in 1331+170 contain predominantly H I region lines. Systems *K* (PHL 957) and *C* (1331+170) contain higher ionizations (e.g., Si IV, C IV, but not N V). The major difference between the objects is that the $D \sim 1.11$ system in 1331+170 is itself split into two systems with a velocity spread of 1000 km s^{-1}, apparently line-locked on Mg II. The possible excess of Lα–Lβ pairs in PHL 957 near the system *A* redshift may be evidence of analogous phenomena in this object. In any event, the most probable redshift systems in the only two objects known to have comparable Lα absorptions have such similar velocity and ionization characteristics that some systematic effect is indicated. The fact that the displacement factors correspond to H or He II resonance transition ratios is also suggestive. This situation has been predicted to occur if matter is being ejected from the QSO under the influence of radiation pressure (Scargle, Caroff, and Noerdlinger 1970; Mushotzky, Solomon, and Strittmatter 1972). The observations of PHL 957 and 1331+170 are, we believe, further evidence that this type of mechanism is operating in quasars.

V. SUMMARY

The results of our study of PHL 957 may be summarized as follows:

i) The profiles of the strongest emission lines in PHL 957 are all different and give rise to uncertainties of order (1–3) × 10^3 km s^{-1} in determining the emission redshift.

ii) The density of absorption lines shortward of the Lα emission is approximately 10 times greater than at longer wavelengths. Most of these absorption lines are thought to be due to clouds with approximately unit Lα optical depth. More than 100 such cloudlets are required in the line of sight to PHL 957.

iii) Only two highly probable redshift systems have been found, the well known system *A* ($z = 2.3088$) and a new system *K* ($z = 1.7969$). These systems are similar to the absorption systems in 1331+170 in both ionization and relative redshift compared with the emission system. This may constitute evidence for line-locking, probably of He II Lα and Lβ on the He II Lyman continuum. This would require an optically thick He II continuum.

iv) No He II λ1640 emission or N V absorption in system *A* or *K* has been detected. The question of

[2] The N V doublet was, in fact, identified by Bahcall, Joss, and Lynds (1973), but the line at 4482 Å identified by them as N V λ1238.8 does not appear in our spectra nor in the high-dispersion LMZOS spectrum.

whether N v emission is present remains unanswered. The results are consistent, however, with the hypothesis that there is a deficiency of He II ionizing photons.

v) Absorption system *A* is consistent with that expected from a pure H I region, although there is marginal evidence for the presence of somewhat higher ionization states (e.g., C III, N II). The system is in fact remarkably similar to the "interstellar" spectra observed in O or B stars (cf. Morton *et al.* 1973) and as such remains a prime candidate as a system arising in an intervening galaxy. An intrinsic origin of this system can certainly not be ruled out, however, especially in view of the increasing evidence that much of the "interstellar" absorption spectrum in early-type stars arises from circumstellar material (Steigman, Strittmatter, and Williams 1975; Castor, McCray, and Weaver 1975).

This work has been supported by the NSF through contracts MPS 71-0343A02 (Steward) and GP-29684 (Lick) and by NATO through contract N0647.

REFERENCES

Arons, J. 1972, *Ap. J.*, **172**, 553.
Bahcall, J. N. 1966, *Ap. J.*, **145**, 684.
———. 1968, *ibid.*, **153**, 679.
———. 1971, *A.J.*, **76**, 283.
Bahcall, J. N., and Joss, P. C. 1973, *Ap. J.*, **179**, 381.
Bahcall, J. N., Joss, P. C., and Cohen, J. G. 1972, *Ap. J.*, **184**, 57.
Bahcall, J. N., Joss, P. C., and Lynds, C. R. 1973, *Ap. J. (Letters)*, **182**, L95.
Bahcall, J. N., and Wolf, R. A. 1968, *Ap. J.*, **152**, 701.
Beaver, E. A., Burbidge, E. M., McIlwain, C. E., Epps, H. W., and Strittmatter, P. A. 1972, *Ap. J.*, **178**, 95.
Blumenthal, G. R., and Mathews, W. G. 1975, *Ap. J.*, **198**, 517.
Carswell, R. F., Hilliard, R. L., Strittmatter, P. A., Taylor, D. J., and Weymann, R. A. 1975, *Ap. J.*, **196**, 351.
Castor, J., McCray, R., and Weaver, R. 1975, *Ap. J. (Letters)*, **200**, L107.
Cowley, E. R., and Aller, M. F. 1972, *Ap. J.*, **175**, 677.
Davidson, K. 1972, *Ap. J.*, **171**, 213.
Grewing, M., and Strittmatter, P. A. 1973, *Astr. and Ap.*, **28**, 39.
Havnes, O., and van den Heuvel, E. P. J. 1972, *Astr. and Ap.*, **19**, 283.
Lowrance, J. O., Morton, D. C., Zucchino, P., Oke, J. B., and Schmidt, M. 1972, *Ap. J.*, **171**, 233 (LMZOS).
Lynds, C. R. 1971, *Ap. J.*, **164**, 673.
MacAlpine, G. M. 1974, *Ap. J.*, **193**, 37.
Morton, D. C., Drake, J. F., Jenkins, E. B., Rogerson, J. B., Spitzer, L., and York, D. G. 1973, *Ap. J. (Letters)*, **181**, L103.
Morton, D. C., and Morton, W. A. 1972, *Ap. J.*, **174**. 237.
Morton, D. C., and Smith, W. H. 1973, *Ap. J. Suppl.*, **26**, 333.
Mushotzky, R. F., Solomon, P. M., and Strittmatter, P. A. 1972, *Ap. J.*, **174**, 7.
Osterbrock, D. E. 1970, *Ap. J.*, **160**, 25.
Ptak, R., and Stoner, R. E. 1973, *Ap. J. (Letters)*, **179**, L89.
Robinson, L. B., and Wampler, E. J. 1972, *Pub. A.S.P.*, **84**, 161.
Russell, H. N., and Bowen, I. S. 1929, *Ap. J.*, **69**, 196.
Scargle, J. D., Caroff, L. J., and Noerdlinger, P. D. 1970, *Ap. J. (Letters)*, **161**, L115.
Spitzer, L., Drake, J. F., Jenkins, E. B., Morton, D. C., Rogerson, J. B., and York, D. G. 1973, *Ap. J. (Letters)*, **181**, L116.
Steigman, G., Strittmatter, P. A., and Williams, R. E. 1975, *Ap. J.*, **198**, 575.
Wiese, W. L., Smith, M. W., and Glennon, B. M. 1966, NSRDS-NBS4.
Wiese, W. L., Smith, M. W., and Miles, B. M. 1969, NSRDS-NBS22.
Williams, R. E. 1971, *Ap. J. (Letters)*, **167**, L27.
———. 1972, *Ap. J.*, **178**, 105.
Williams, R. E., Strittmatter, P. A., Carswell, R. F., and Craine, E. R. 1975, *Ap. J.*, **202**, 296.
Wingert, D. W. 1975, *Ap. J.*, **198**, 267.

J. BALDWIN, L. B. ROBINSON, and E. J. WAMPLER: Lick Observatory, University of California, Santa Cruz, CA 95064

R. F. CARSWELL: Department of Physics, University College London, Gower Street, London WC1E 6BT, England

G. COLEMAN, P. A. STRITTMATTER, and R. E. WILLIAMS: Steward Observatory, University of Arizona, Tucson, AZ 85721

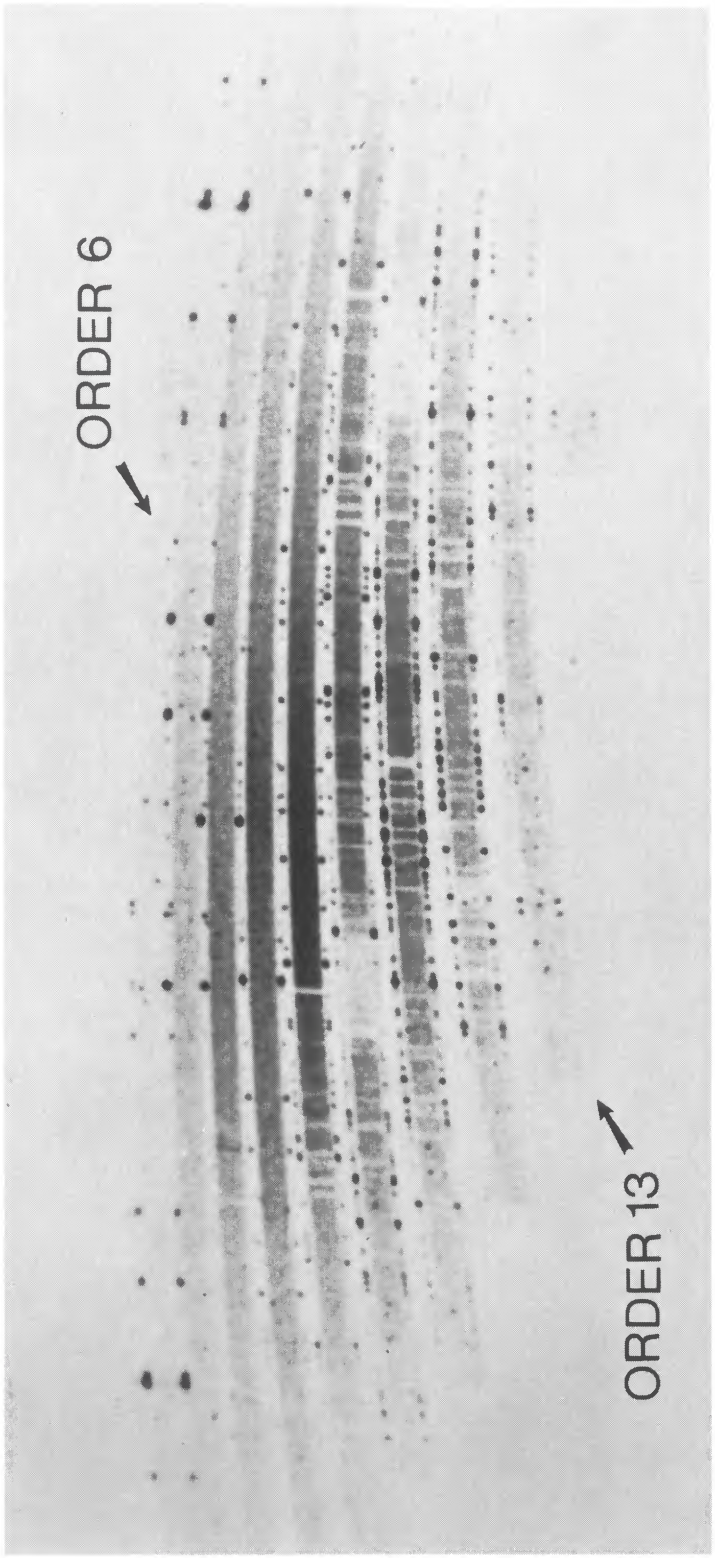

FIG. 2.—Steward echelette spectrogram (SI1525) of PHL 957. The exposure time was 55^{m} on IIaO emulsion behind the RCA 33063 image intensifier, and the widening is 0.4 mm.